Identification of the major functional proteins of prokaryotic lipid droplets[S]

Yunfeng Ding,[1,*,†] Li Yang,[1,*,†] Shuyan Zhang,* Yang Wang,*[,†] Yalan Du,*[,§] Jing Pu,*[,†] Gong Peng,*[,†] Yong Chen,* Huina Zhang,* Jinhai Yu,*[,†] Haiying Hang,* Peng Wu,* Fuquan Yang,* Hongyuan Yang, Alexander Steinbüchel,[2,††] and Pingsheng Liu*[,2]**

National Laboratory of Biomacromolecules, Institute of Biophysics, Beijing, China;* Graduate University of Chinese Academy of Sciences, Beijing, China;[†]Department of Histology and Embryology, University of South China, Hengyang, Hunan Province, China;[§] School of Biotechnology and Biomolecular Sciences, University of New South Wales, Sydney, Australia;** and Institut für Molekulare Mikrobiologie und Biotechnologie, Westfälische Wilhelms-Universität, D-48149 Münster, Germany, and King Abdulaziz University, Jeddah, Saudi Arabia[††]

Abstract Storage of cellular triacylglycerols (TAGs) in lipid droplets (LDs) has been linked to the progression of many metabolic diseases in humans, and to the development of biofuels from plants and microorganisms. However, the biogenesis and dynamics of LDs are poorly understood. Compared with other organisms, bacteria seem to be a better model system for studying LD biology, because they are relatively simple and are highly efficient in converting biomass to TAG. We obtained highly purified LDs from *Rhodococcus* sp. RHA1, a bacterium that can produce TAG from many carbon sources, and then comprehensively characterized the LD proteome. Of the 228 LD-associated proteins identified, two major proteins, ro02104 and PspA, constituted about 15% of the total LD protein. The structure predicted for ro02104 resembles that of apolipoproteins, the structural proteins of plasma lipoproteins in mammals. Deletion of ro02104 resulted in the formation of supersized LDs, indicating that ro02104 plays a critical role in cellular LD dynamics. The putative α helix of the ro02104 LD-targeting domain (amino acids 83–146) is also similar to that of apolipoproteins. JLR **We report the identification of 228 proteins in the proteome of prokaryotic LDs, identify a putative structural protein of this organelle, and suggest that apolipoproteins may have an evolutionarily conserved role in the storage and trafficking of neutral lipids.**—Ding, Y., L. Yang, S. Zhang, Y. Wang, Y. Du, J. Pu, G. Peng, Y. Chen, H. Zhang, J. Yu, H. Hang, P. Wu, F. Yang, H. Yang, A. Steinbüchel, and P. Liu. **Identification of the major functional proteins of prokaryotic lipid droplets. *J. Lipid Res.* 2012.** 53: **399–411.**

Supplementary key words Rhodococcus RHA1 • microorganism lipid droplet small • proteomics • apolipoprotein

Lipid droplets (LDs) are intracellular organelles with neutral lipid cores surrounded by a phospholipid monolayer and coated with various proteins (1–3). LDs have been found in almost all eukaryotic organisms from yeast to mammals (4). They interact with other cellular organelles (5–8), and their dynamics is closely related to the progression of metabolic diseases, such as obesity, fatty liver, type 2 diabetes mellitus, and atherosclerosis (9). Recent studies have also shown that LDs are involved in the reproduction of infectious hepatitis C virus particles (10) and in protecting cells from damage (11). The identification of perilipin, ADRP, and Tip47 (PAT) family proteins has provided useful marker proteins to facilitate the purification of LDs. Recent proteomic studies suggesting that LDs are not simply inert cellular inclusions for the storage of neutral lipids, but rather functional cellular organelles, has established a new era in LD research (3, 12–18).

Although LDs are highly dynamic organelles involved in many cellular activities, especially lipid metabolism, the molecular mechanisms that govern LD formation remain largely unknown. The current model of LD biogenesis speculates that LDs are derived from the endoplasmic reticulum (ER) by a process that begins with the accumulation of neutral lipids between the leaflets of phospholipid bilayers (3, 19). Many studies have attempted to unravel how LDs form and grow, but this hypothesis still lacks direct evidence and the molecular mechanism

This work was supported by grants from the Ministry of Science and Technology of China (Grant 2009CB919000, Grant 2010CB833703; Grant 2011CBA00900), and the National Natural Science Foundation of China (Grant 30871229, Grant 30971431, and Grant 31000365). The authors declare that there are no competing financial interests.

Manuscript received 26 October 2011 and in revised form 15 December 2011.

Published, JLR Papers in Press, December 15, 2011
DOI 10.1194/jlr.M021899

Abbreviations: ER, endoplasmic reticulum; LD, lipid droplet; MLDS, microorganism lipid droplet small; MSM, mineral salt medium; NB, nutrient broth; PAT, perilipin, ADRP, and Tip47; PspA, phage shock protein A; TAG, triacylglycerol; TEM, transmission electron microscopy.

[1]Y. Ding and L. Yang contributed equally to this article.
[2]To whom correspondence should be addressed.
e-mail: alexander.steinbuechel@uni-muenster.de (A.S.);
pliu@sun5.ibp.ac.cn (P.L.)

[S] The online version of this article (available at http://www.jlr.org) contains supplementary data in the form of five figures and six tables.

underlying LD formation remains unknown (20–25). In addition to their association with metabolic diseases, LDs also have potential to be exploited in the development of biofuels (26). For example, biodiesel can be generated from triacylglycerols (TAGs) that are stored in the LDs of plants and microorganisms (27, 28). Therefore, determining how LDs form and identifying proteins that affect LD size will facilitate our understanding of metabolic diseases and also enhance our ability to develop green biodiesels.

Prokaryotic organisms are of interest in development of biofuel, and insights into their LDs may facilitate eukaryotic LD study. We used the Gram-positive bacterium *Rhodococcus* sp. RHA1, whose genome has recently been sequenced (29) and in which the LD is the only organelle, as a model system. *Rhodococcus* sp. RHA1 was originally collected from lindane-contaminated soil. It utilizes a wide range of organic compounds as carbon sources, such as carbohydrates, sterols, aromatic compounds, and nitriles. Recent investigations of RHA1 have mainly focused on its potential use in treating contaminated soil and water through its biodegradation of pollutants such as eugenol, nitrile, 7-ketocholesterol, benzoate, phthalate (30–32), cellulose, hemicellulose, and lignin (33). This bacterium accumulates TAG to a very high level, and is a potential renewable source for biofuel production.

Several studies on bacterial LD proteins have been reported previously, but the detailed protein composition of LDs is still unknown. PAT family proteins, considered to be the structural proteins of LDs, can be detected in organisms from *Drosophila* to humans (3, 34, 35). However, although *Caenorhabditis elegans*, yeast, and certain bacteria possess similar cellular organelles, they appear to lack this family of structural proteins. Absence of these LD marker proteins has hampered the purification of LDs from these organisms.

Here we established a method for purifying lipid droplets from bacteria and carried out a proteomic study to identify LD-associated proteins, thereby exploring LD formation and function. We demonstrated that or02104, one of the 228 LD-associated proteins identified in this study, plays an important role in determining LD size and has significant structural similarity to apolipoproteins. Therefore, we designated it as microorganism lipid droplet small (MLDS). This work will have potential impact on LD biology for both prokaryotic and eukaryotic organisms.

MATERIALS AND METHODS

Strains and culture conditions

The bacterial strains and plasmids used in this study are listed (see supplementary Table I). Cells of *Rhodococcus* sp. RHA1 were cultivated aerobically in nutrient broth (NB) in Erlenmeyer flasks at 30°C. To promote accumulation of TAGs, 40 ml of cells (OD600 = 2.0) was harvested by centrifugation and then cultivated for 24 h in 400 ml mineral salt medium (MSM) with 0.5 g/l NH_4Cl as a nitrogen source and 10 g/l gluconate sodium as a carbon source.

Confocal microscopy

Cultivated RHA1 cells were washed twice with PBS. Cells were then dropped on cover glasses pretreated with rat tail collagen and allowed to dry for 30 min before washing with 1 ml PBS. Cells were incubated in a 1:500 solution of Lipid-TOX Deep Red (H34477) in darkness for 30 min. Samples were mounted on glass slides using Mowiol mounting media and viewed with an Olympus FV1000 confocal microscope.

TLC

Bacterial samples were extracted twice with a mixture of chloroform-methanol-medium (1:1:1, v/v/v). Purified LDs were extracted by chloroform-acetone (1:1, v/v). Organic phases were collected and dried under high-purity nitrogen gas. Total lipids were dissolved in 100 μl chloroform, vortexed, and centrifuged for 1 min at 10,000 rpm. Samples were then subjected to TLC analysis with Whatman Purasil™ 60FÅ silica gel plates (Merck; Germany). Plates were developed in a hexane-diethyl ether-acetic acid (80:20:1, v/v/v) solvent system to separate neutral lipids, and in chloroform-methanol-acetic acid-H_2O (75:13:9:3, v/v/v/v) to detect phospholipids. Plates were visualized using iodine vapor and quantified by grayscale scanning (NIH ImageJ software).

Isolation of lipid droplets

A previously reported method (12, 18) was modified and used to isolate lipid droplets from bacteria. RHA1 cells cultivated in MSM were harvested by centrifugation at 3,000 *g* for 10 min in a 50 ml tube (Sigma 12150-H), washed twice with 30 ml buffer A (25 mM tricine, 250 mM sucrose, pH 7.8), and resuspended in 30 ml buffer A. After 20 min incubation on ice, cells were homogenated by passing through a French pressure cell three times at 100 MPa, 4°C. The sample was centrifuged in a 50 ml tube at 3,000 *g* for 10 min to remove cell debris. Supernatant (8 ml) was loaded into each SW40 tube with 2 ml buffer B (20 mM HEPES, 100 mM KCl, 2 mM $MgCl_2$, pH 7.4) on top, and was then centrifuged at 182,000 *g* for 1 h at 4°C (Beckman SW40). The LD fraction on top of the sucrose gradient was collected using a 200 μl pipette tip and transferred to a 1.5 ml Eppendorf tube. LDs were washed three times with 200 μl Buffer B until there was no visible pellet at the bottom of the tube. During this process, the solution underlying the LD layer was removed using a gel-loading tip. One milliliter chloroform-acetone (1:1, v/v) was added to dissolve lipids and to precipitate proteins. The sample was vortexed adequately and centrifuged at 20,000 *g* for 10 min (Eppendorf centrifuge 5417R). The pellet was dissolved with 50 μl 2×SDS sample buffer, and the sample was then denatured at 95°C for 5 min and stored at −20°C for further analysis (see supplementary Fig. I).

MS analysis

Lipid droplet proteins were separated on a 10% SDS-PAGE gel and subjected to silver staining. The lane with LD proteins was cut into 43 slices. In-gel digestion of each slice was performed as follows. Each slice was successively destained with 15 mM $FeK_3(CN)_6$ and 50 mM $Na_2S_2O_3$, and then dehydrated with 100% acetonitrile. Proteins were reduced with 10 mM DTT in 25 mM ammonium bicarbonate at 56°C for 1 h and alkylated by 55 mM iodoacetamide in 25 mM ammonium bicarbonate in the dark at room temperature for 45 min. Finally, gel pieces were thoroughly washed with 25 mM ammonium bicarbonate in water-acetonitrile (1:1, v/v) solution and completely dried in a SpeedVac. Proteins were incubated for 30 min in 10 μl of modified trypsin solution (10 ng/ml in 25 mM ammonium bicarbonate) on ice before adding 25 μl of 25 mM ammonium bicarbonate and leaving overnight at 37°C. The digestion reaction was stopped by addition of 2% formic acid to give a final concentration of 0.1%. The

gel pieces were extracted twice with fresh 80 μl 60% acetonitrile plus 0.1% formic acid, and then sonicated for 10 min. All liquid samples from the three extractions were combined and dried in a SpeedVac (ThermoFisher Scientific; Germany).

Dried peptide samples were dissolved in 20 μl 0.1% formic acid, loaded onto a C_{18} trap column with an autosampler, eluted onto a C_{18} column (100 mm × 100 μm) packed with Sunchrom packing material (SP-120-3-ODS-A, 3 μm), and then subjected to nano-LC-ESI-LTQ MS/MS analysis. The quadrupole linear ion trap (LTQ) mass spectrometer was operated in data-dependent mode with the initial MS scan ranging from 400 to 2,000 Da. The five most-abundant ions were automatically selected for subsequent collision-activated dissociation.

All MS/MS data were searched against the RHA1 protein database downloaded from the *Rhodococcus* Genome Project website (http://www.rhodococcus.ca) using the SEQUEST program (Thermo, USA). BioWorks search parameters were set as follows: enzyme: trypsin; precursor ion mass tolerance: 2.0 Da; and fragment ion mass tolerance: 1.0 Da. The variable modification was set to oxidation of methionine (Met + 15.99 Da). The fixed modification was set to carboxyamidomethylation of cysteine (Cys + 57.02 Da). The search results were filtered with Xcorr vs. Charge values of Xcorr (+ 1) > 2.0, Xcorr (+ 2) > 2.5, and Xcorr (+ 3) > 3.5.

Antibody preparation

Twenty lipid droplet proteins identified by proteome analysis were selected for antibody production. For each protein, two rabbits were immunized with a mixture of two synthetic peptides. After three injections, the rabbit sera were tested using Western blotting. In this way, 10 usable antibodies were generated (Fig. 3).

Western blotting

Bacteria and LD proteins were lysed directly using 2×SDS sample buffer, sonicated twice for 9 s each time at 200 watts, and denatured at 95°C for 5 min, followed by a brief centrifugation at 10,000 *g*. Total proteins were separated by SDS-PAGE, transferred to a polyvinylidene difluoride membrane, blotted using the antibodies indicated, and detected using an ECL system.

Construction of the ro02104 and *pspA* deletion mutants

Construction of these mutants is described (see supplementary Fig. II).

Transmission electron microscopy

Bacterial cells and isolated lipid droplets were subjected to negative staining and ultra-thin sectioning, and examined by transmission electron microscopy (TEM). For negative staining, isolated lipid droplets were placed on a Formvar-carbon coated copper grid and stained for 30 s by adding an equal volume of 2% (w/v) uranyl acetate. The grid was then viewed with a FEI Tecnai 20 electron microscope (FEI Co., Netherlands). For negative staining of bacterial cells, samples were loaded on carbon-coated copper grids. Subsequently 2% (w/v) phosphotungstic acid was used to stain the sample for 2 min. The grid was then washed three times with deionized water before viewing with an electron microscope. Bacterial cells were prepared for ultra-thin sectioning as follows. Samples were prefixed in 2.5% (w/v) glutaraldehyde in PBS (pH 7.4) overnight at 4°C and postfixed in 1% (w/v) osmium tetroxide for 24 h at 4°C. Dehydration was carried out in an ascending concentration series of ethanol at room temperature. Samples were then embedded in Quetol 812 and sectioned to a thickness of 90 nm with a Leica EM UC6 Ultramicrotome (Leica Germany). Sections were stained with 2% (w/v) uranyl acetate for 15 min and with lead citrate for 5 min at room temperature. Stained sections were examined with an electron microscope.

Measurement of TAG levels

The same quantity of RHA1 wild-type (WT) and MLDS deletion mutant cells were transferred to MSM after culturing in NB. Cell suspension samples (1 ml) were withdrawn at different time points. Cells were washed twice with l ml PBS, then dissolved in 200–400 μl 1% Triton X-100 by sonication. Whole-cell lysates were then centrifuged at 10,000 *g* for 5 min at 4°C. The TAG content of the supernatant was measured using an E1003 triglyceride assay kit (Applygen Technologies; China). Protein concentration was quantified using a Pierce BCA Protein Assay Kit (Thermo, USA).

Construction of green fluorescent protein fusion proteins

Different MLDS truncations and ro05869 were amplified without their native start and stop codons using the primers shown (see supplementary Table II). These truncations were then respectively cloned into the *Bam*HI site of pJAM2-*egfp*. Plasmids were transformed into RHA1 using a Bio-Rad 165-2100 MicroPulser (Bio-Rad, USA). Electro-competent cells of RHA1 were prepared according to Kalscheuer, Arenskötter, and Steinbüchel (36).

RESULTS

Isolation of LDs from *Rhodococcus* sp. RHA1

In this study, cells were cultivated in either NB to promote division and growth or in MSM containing a growth-limiting amount of nitrogen, and an excess amount of sodium gluconate as a carbon source to promote TAG accumulation. Lipid-TOX staining showed that RHA1 cells cultivated in NB formed small LDs, whereas in cells cultivated in MSM, LDs were much larger (**Fig. 1A**). TLC analysis verified this finding by showing that the amount of TAG in cells cultivated in MSM was significantly higher than that in cells cultivated in NB (Fig. 1B). LDs were isolated from cells cultured in MSM (see supplementary Fig. I). After ultracentrifugation, LDs floated to the top of the sucrose gradient and cell membranes pelleted at the bottom of the tube (Fig. 1C). To better visualize LDs in this bacterium, cells were cultivated in MSM and imaged by TEM after ultra-thin sectioning. Electron microscopy images clearly show that there are many LDs in RHA1 (Fig. 1D).

The purity of isolated LDs is very critical for obtaining an accurate proteomic analysis. The best way to determine the purity of LDs would be by the enrichment of LD-marker proteins such as the PAT family proteins found in mammalian cells. However, the major/structural proteins of LDs in organisms from bacteria to *C. elegans* that could be used as LD markers still need to be identified; their identification is one of the specific aims of this study. In the absence of such markers, then, we used the following six steps to verify the purity of LD preparations based on methods we had developed previously (12, 18). First, LDs isolated from RHA1 were examined by negative staining and imaged by TEM. The images verified that there was almost no membrane contamination in the LD preparations (Fig. 1D). Second, purified LDs were analyzed with a

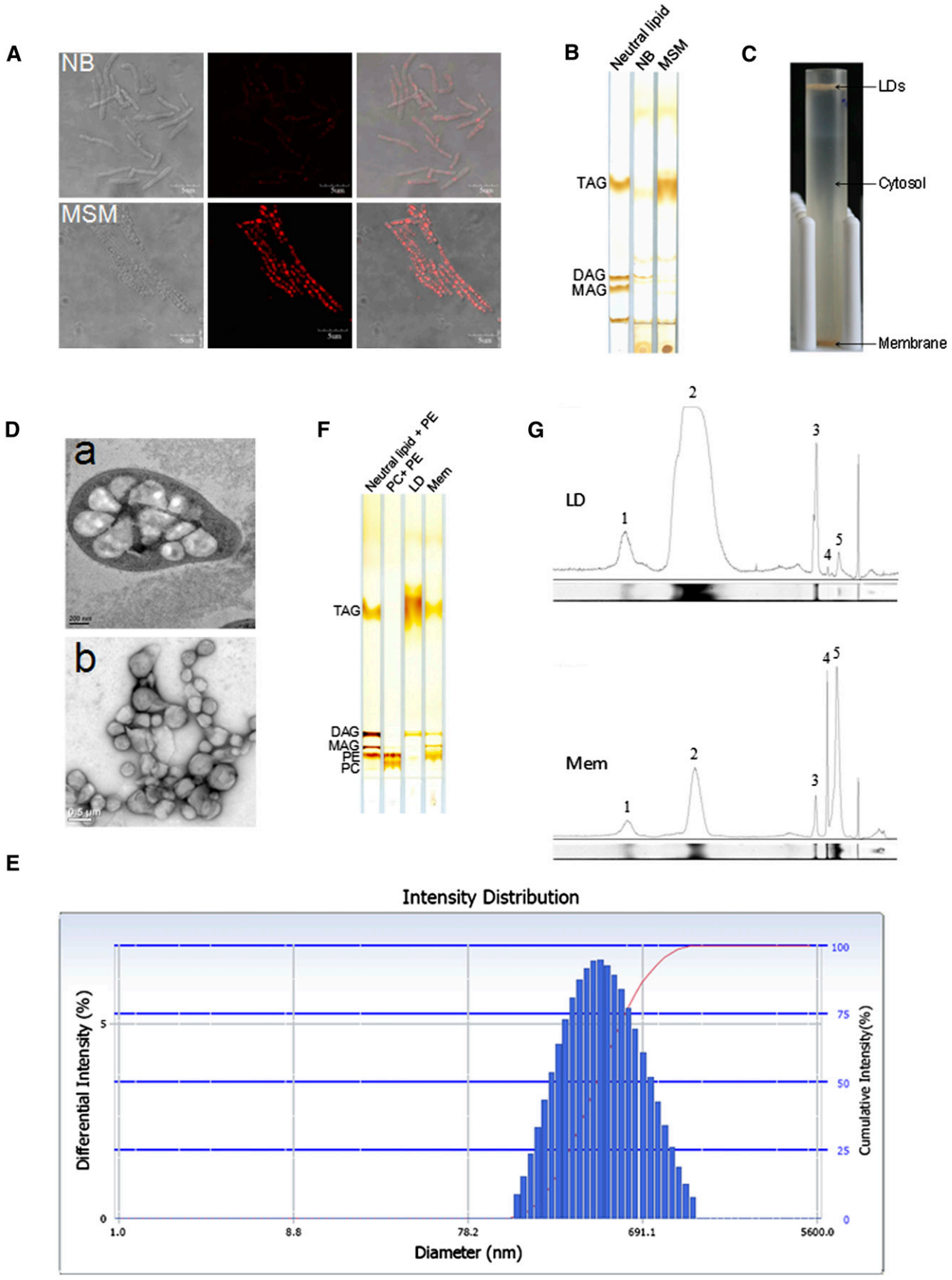

Fig. 1. Isolation of lipid droplets from *Rhodococcus* sp. RHA1. A: Cells of strain RHA1 cultivated in NB and MSM were stained by LipidTOX and imaged by confocol microscopy. Left panel, the phase-contrast images; middle, the corresponding fluorescence images; right panel, the merged images. Bar = 5 μm. B: Total lipids were extracted from NB and MSM cultures (quantities normalized by protein concentration) and subjected to TLC analysis. C: RHA1 cells cultivated in MSM were collected and homogenized. After removal of cell debris,

Delsa Nano C particle analyzer. LD size was distributed as a bell-shaped normal distribution ranging between 220 nm and 690 nm (Fig. 1E), indicating that isolated LDs were the intracellular structures visualized by EM previously. Third, protein profiles were obtained from three separate LD isolations and were almost identical (see supplementary Fig. IIIA). Fourth, total lipids were extracted from purified LDs and cell membranes, and separated by TLC along with standards (Fig. 1F). TLC results showed that LDs were highly enriched in TAG. Small amounts of diacylglycerol (DAG), unknown neutral lipid, phosphatidylethanolamine (PE), and monoacylglycerol (MAG) were also detected (Fig. 1G). Total membrane fractions were enriched in PE. Small amounts of TAG, DAG, MAG, and unknown neutral lipids were detected (Fig. 1G). Fifth, Colloidal Blue staining of LDs revealed that their protein composition was distinctly different from that of the proteins of the total membrane, cytosol, and whole-cell lysate fractions (**Fig. 2A**). The LD protein profile contained four major bands, which accounted for nearly 40% of all LD-associated proteins. Sixth, protein profiles from LDs washed three, six, and nine times were the same (see supplementary Fig. IIIB). Taken together, these results confirm that our LD preparations were of high purity and therefore suitable for further proteomic analysis.

Analysis of the RHA1 LD proteome

Proteins were then extracted from purified LDs and subjected to proteomic analyses. To avoid missing low-abundance and/or nonstainable proteins and to utilize molecular weight as a criterion for proteomic analysis, total proteins were separated by SDS-PAGE and visualized using silver staining; the whole lane of LD proteins from cells cultivated in MSM was then cut into 43 slices according to visible protein bands, and each slice was subjected to proteomic analysis (Fig. 2B). To improve reliability, two LD preparations prepared in an identical manner were analyzed separately and compared with each other (Fig. 2C). Four hundred twenty-nine LD proteins were found in the first preparation (see supplementary Table III), whereas 402 proteins were found in the second preparation (see supplementary Table IV). Only proteins present in both preparations were considered to be putative LD proteins. Two hundred twenty-eight proteins were identified in both proteomic analyses, including 149 enzymes, 18 transcriptional regulators, 11 ribosome proteins, 5 cell division-related proteins, 3 stress response proteins, 2 chaperones, and 40 other proteins, including 16 of unknown function (Fig. 2D; see supplementary Table V). To provide a greater understanding of LD-associated protein dynamics, these results were compared with a proteomic analysis performed on cells cultured in NB. The main LD protein bands from cells cultured in NB (Fig. 2B, bands 44 to 48) were similarly subjected to LC-MS analysis. Most LD proteins identified from these bands were basically identical to those in LDs from cells grown in MSM. However, the abundance of some proteins appeared to be different under these two conditions, as judged from the number of peptides (**Table 1**). Most proteins, such as the 60 kDa chaperonin GroEL (GI 111019139) and a chaperone protein (GI 111023153) were abundant in both NB and MSM, whereas the expression of some proteins, such as a possible phage shock protein (GI 111023715) and an adenylate cyclase family protein (GI 111021861) was enhanced, and the expression of other proteins, such as an apolipoprotein-like protein (GI A1/A4/E 111019097) was reduced. The functional associations of the overlapped 228 proteins were drawn as a network (see supplementary Fig. IV) using STRING 9.0 with default parameters (37). More than 76 proteins that are mainly involved in biosynthetic process form a dense cluster in the network. A detailed gene ongology functional clustering of these genes was analyzed by using DAVID (38, 39). Eighteen of them are related to protein translation; 19 of them are involved in nitrogen compound biosynthesis; 10 of them are responsible for amine biosynthesis; 9 of them are involved in amino acid biosynthetic process; 10 of them are related to carboxylic acid biosynthesis; and 10 of them are related to organic acid biosynthesis (see supplementary Table VI). It is not clear whether the LD-associated proteins are synthesized by these proteins. However, the occurrence of so many proteins involved in biosynthesis on the surface of lipid droplets suggests that LDs may serve as a surface where many important bioprocesses are carried out. These results are also consistent with earlier proteomic studies (5).

Verification of proteins identified by proteomics

To verify the proteomic results and to determine the distribution of these proteins in cells, antibodies against abundant LD proteins were generated in our laboratory. Equal amounts of proteins from LD, total membrane, cytosol, and whole-cell lysate fractions were separated by SDS-PAGE (**Fig. 3F**). Proteins tested (Fig. 3A–D) were found to be enriched in the LD fraction as determined by Western blotting. The high level of enrichment of these proteins in LDs further confirms the high quality of the isolated LDs. Furthermore, the results of Western blotting showed the cellular distribution of these proteins. For example, ro05869, ro00061, ro04894, ro02104, ro06757, ro01247, and ro02146 occurred mainly in the LD fraction,

whole-cell lysate ultracentrifugation was performed at 182,000 *g* for 1 h at 4°C (Beckman SW40). The lipid droplet fraction floated to the top of the sucrose gradient while the total membrane fraction remained at the bottom. D: D-a, ultra-thin sections of RHA1 cultivated in MSM and imaged by EM (bar = 0.2 μm). D-b, isolated LDs imaged by EM after negative staining (bar = 0.5 μm). E: Purified LDs were collected from the top of the sucrose gradient in the SW40 tube, and then analyzed with a Delsa Nano C particle analyzer. The distribution of LD intensity according to diameter is shown. F: Total lipids were extracted from purified LD and total membrane fractions, respectively, followed by TLC analysis. The TLC plate was visualized by iodine vapor. G: The lipid content was semi-quantified by grayscale scanning (NIH ImageJ software). The area under the peak reflects the content of each component. 1, unknown neutral lipid; 2, TAG; 3, DAG; 4, MAG; 5, PE.

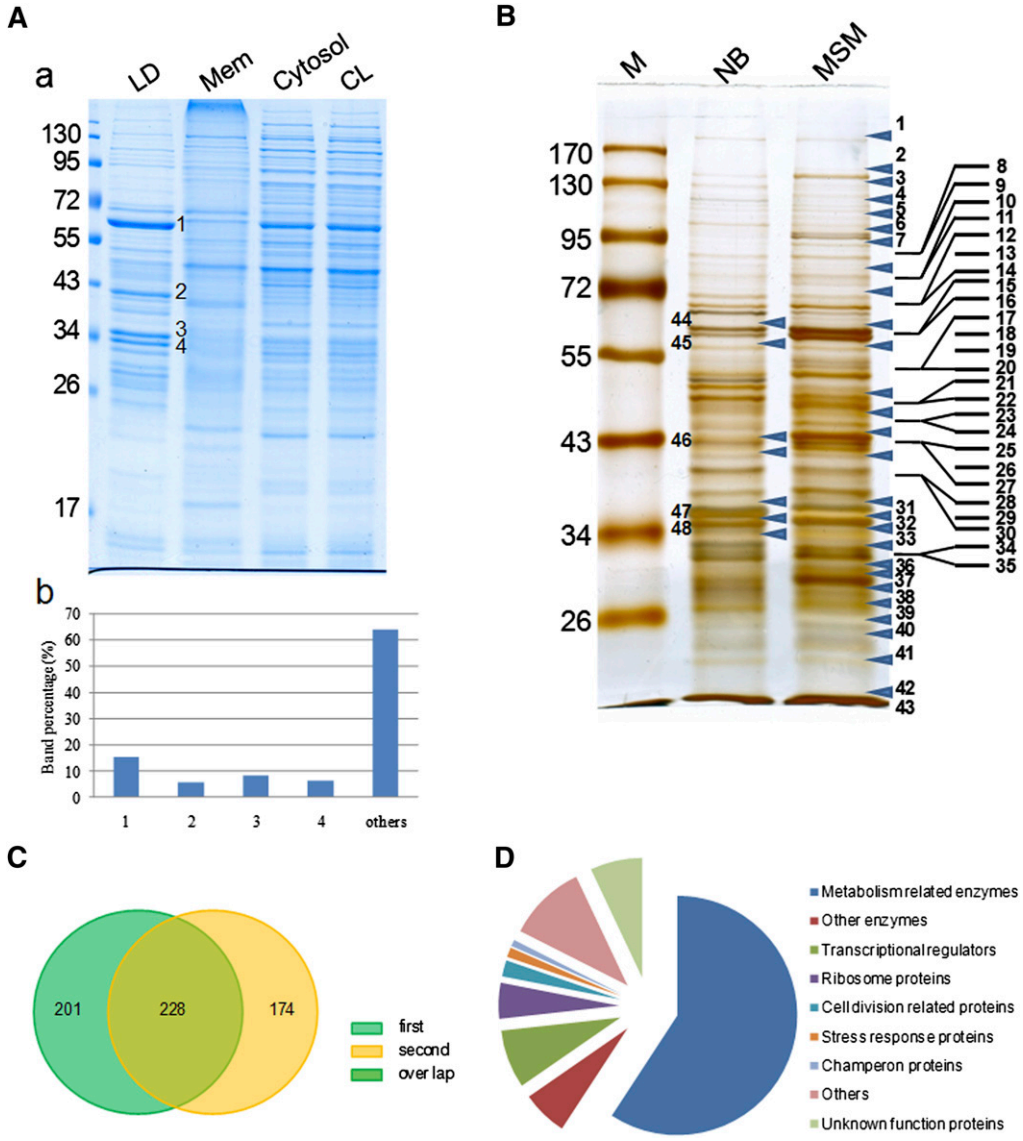

Fig. 2. Analysis of LD-associated proteins by proteomics and bioinformatics. A: A-a, RHA1 cells cultivated in MSM were collected and fractionated as described in MATERIALS AND METHODS. Proteins from purified lipid droplets (LD), membrane (Mem), cytosol, and whole-cell lysates (CL) were separated by 10% SDS-PAGE followed by Colloidal Blue staining. A-b, bands in the LD protein lane were quantified by gray-scale scanning (Alpha Ease Fluor Chem). The table shows the ratio of the main bands: 1: 15.4%; 2: 5.8%; 3: 8.2%; 4: 6.4%. B: LD protein bands were analyzed by LC-MS. Forty-three bands from the MSM sample lane, and the five bands from the NB sample corresponding to the major bands in the MSM sample were analyzed. Arrows indicate the positions at which the gel was sliced. C: To improve the reliability of our analysis of LD proteins, two samples were analyzed separately by LC-MS. Two hundred twenty-eight LD-associated proteins were present in both samples of RHA1 cells cultivated in MSM. D: The 228 LD-associated proteins were categorized into nine groups after searching against the RHA1 genome, Pfam, and NCBI databases.

whereas ro02258 and ro06190 occurred in both the LD and the cytosol fraction. The functions of these proteins were identified by Pfam motif searching; ro04894 (Fig. 3B) is an adenylate cyclase that is involved in the production of cyclic AMP, and ro02258 is a FA desaturase that occurs not only on LDs but also in the cytosol (Fig. 3D). ro00061, ro06757, and ro01247 were identified as stress response proteins, suggesting that LDs may play a role when cells encounter a harsh environment (Fig. 3C, D). The function of ro05869 could not be identified (Fig. 3A), and it remains a hypothetical protein. The enrichment of bacterial chaperone proteins ro02146 and ro06190 identified here is consistent with reports on the enrichment of chaperone proteins in the LD fraction of mammalian cells (18). The dynamin-like protein ro05469 was not detected in our proteomic analysis of LD proteins, but was shown by Western blotting to be present in the membrane and cytosol fractions, providing further evidence that cytosolic contamination was not a problem in our LD preparations (Fig. 3E). To confirm that the Western blotting can indeed reflect the distribution of these proteins, ro05869 GFP fusion protein was overexpressed in RHA1 cells and imaged by

TABLE 1. Comparative proteomics between lipid droplet proteins of RHA1 cultivated in NB and MSM

NB	MSM
Band 44	Band 15
60 kDa chaperonin GroEL (17)	60 kDa chaperonin GroEL (13)
	Chaperone protein (8)
Band 45	Band 16
60 kDa chaperonin GroEL (12)	60 kDa chaperonin GroEL (6)
Chaperone protein (11)	Chaperone protein (21)
	Adenylate cyclase family protein (8)
	Probable uroporphiryn-III C-methyltransferase (3)
Band 46	Band 15–27
IMP dehydrogenase/GMP reductase (7)	IMP dehydrogenase/GMP reductase (10)
Pyruvate kinase (3)	Pyruvate kinase (5)
FA CoA dehydrogenase (3)	Probable UDP-glucose 4-epimerase (6)
	Pyruvate kinase (5)
	Probable As(2+)-transporting ATPase (5)
	Probable linoleoyl-CoA desaturase (4)
	AFG1-like ATPase|RHA1_ro06866 (4)
	Possible hydrolase (4)
	Probable oxidoreductase (4)
	NAD(P) transhydrogenase α subunit (3)
	Probable glutaryl-CoA dehydrogenase (3)
	Acyl CoA dehydrogenase (3)
	Aspartate-semialdehyde dehydrogenase (3)
Band 47	Band 31
Possible phage shock protein (9)	Possible phage shock protein (6)
Apolipoprotein A1/A4/E (9)	Sporulation regulator whiA N-terminal (6)
Sporulation regulator whiA N-terminal (8)	Methyltransferase domain (4)
Diacylglycerol kinase catalytic domain (4)	Glycosyltransferase (7)
30S ribosomal protein S3 (4)	H(+)-transporting two-sector ATPase γ subunit (5)
NAD dependent epimerase/dehydratase (3)	Hypothetical protein (5)
Probable arginine transport ATPase (3)	FeS assembly ATPase (4)
Methyltransferase domain (3)	Ribose-phosphate diphosphokinase (4)
	Recombinase A (3)
	Cell division initiation protein (3)
	α/beta hydrolase of unknown function (3)
	Hypothetical protein (3)
Band 48	Band 32
Possible phage shock protein (11)	Possible phage shock protein (18)
Apolipoprotein A1/A4/E (5)	Ribose-phosphate diphosphokinase (8)
Ribose-phosphate diphosphokinase (4)	Probable short-chain dehydrogenase (5)
Glycosyltransferase (4)	Apolipoprotein A1/A4/E (3)
FeS assembly ATPase (3)	Probable ABC multidrug resistance transporter (3)
	Xylose isomerase-like TIM barrel (3)
	Acyl-[acyl-carrier-protein]desaturase (3)

Lipid droplet proteins were extracted from RHA1 cells cultivated in NB and MSM, respectively. After silver staining, the main bands of lipid droplet protein lanes were cut corresponding to the same position and subjected to LC-MS analysis (Fig. 2B). The numbers in parentheses are peptide numbers identified through LC-MS.

confocal microscopy (Fig. 3G). The confocal microscopy result clearly showed that ro05869 was colocalized with LDs, which was consistent with the Western blotting result. The high expression level of ro02104 in LDs is especially interesting inasmuch as it is a mammalian apolipoprotein-like protein (see supplementary Fig. VA). The secondary structure prediction showed that ro02104 was enriched in α helix as well as human apoA1/A4/E (see supplementary Fig. VB). Therefore, it is possible that this protein might play an important role in LD structure maintenance (Fig. 3D).

ro02104 and PspA are the two major proteins of LDs

PAT family proteins, the main structural proteins of eukaryotic LDs, play important roles in LD function and dynamics. However, their expression has only been detected in organisms from *Drosophila* to humans and has not been found in any prokaryotic organisms. The identification of the major structural proteins in prokaryotic LDs, therefore, is a very important step that will facilitate the study of prokaryotic LDs. Here, the main bands identified on SDS-PAGE gels of LD proteins (Fig. 2A; bands 1–4) were considered as candidate major LD proteins. To test whether the proteins from these bands play a structural role in LDs, we deleted the corresponding genes for bands 3 and 4 by homologous recombination (see supplementary Fig. II) (40, 41). **Figure 4A** presents the diagram of the in-frame deletion of ro02104 (Fig. 4C, band 3) and *pspA* (Fig. 4C, band 4). ro02104 and *pspA* deletions mutants were confirmed by PCR and Western blotting (Fig. 4B). Figure 4C shows that band 3 was absent in the LD proteins from the ro02104 deletion mutant, and that band 4 was markedly reduced in the *pspA* deletion mutant. These results were recapitulated in the ro02104-*pspA* double deletion mutant, indicating that ro02104 (GI 111019097), which shares similarities to apolipoprotein family proteins, and phage shock protein A (PspA) (GI 111023715) are major proteins in RHA1 LDs.

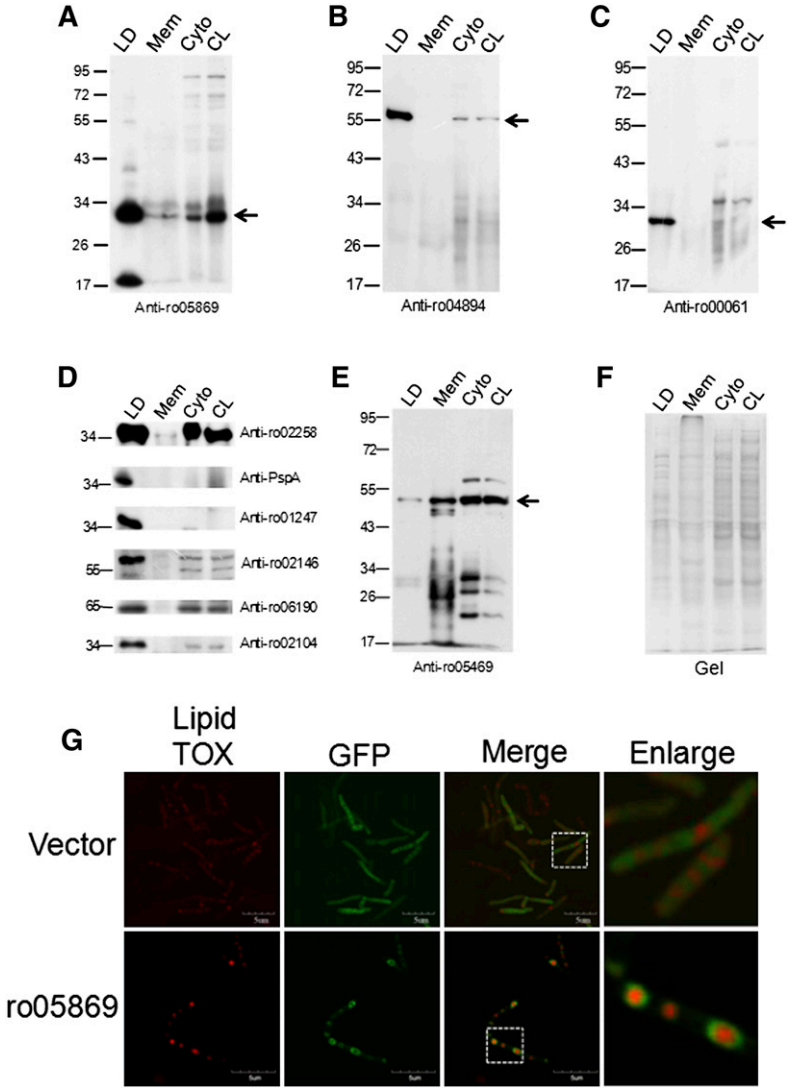

Fig. 3. Western blotting of LD proteins. The same quantity of protein from LDs, membranes (Mem), cytosol (Cyto), and cell lysates (CL) was separated on 10% SDS-PAGE gels and then subjected to Western blotting. Antibodies were generated in rabbits by using synthetic peptides as antigens. A: Western blotting using anti-ro05869; B: Western blotting using anti-ro04894; C: Western blotting using anti-ro00061; D: Western blotting using anti-ro02258, anti-ro06757, anti-ro01247, anti-ro02146, anti-ro06190, or anti-ro02104; E: Western blotting using anti-ro05469; F: Image of the SDS-PAGE gel before Western blotting provides a protein loading control. G: The ro05869 was cloned into pJAM-*egfp* and overexpressed in RHA1 cells after transformation, then imaged by FV1000 confocal microscopy. Upper panels: the vector pJAM–*egfp* overexpressed in RHA1; lower panels: ro05869 overexpressed in RHA1.

Deletion of ro02104 increases the size of LDs

To study the function of these proteins, we first analyzed the phenotypes of the ro02104 and *pspA* deletion mutants, and their double-deletion mutant. The size and shape of LDs in these strains were examined by EM. Interestingly, negative staining images clearly showed that LDs were much larger in cells of the ro02104 deletion mutant (**Fig. 5A**) and the ro02104-*pspA* double-deletion mutant (Fig. 5A), than those in WT (Fig. 5A). No significant change in LD size was observed in the *pspA* deletion mutant (Fig. 5A) compared with the WT (Fig. 5A). Furthermore, the number of LDs decreased dramatically in the ro02104 deletion mutant and the ro02104-*pspA* double deletion mutant, suggesting that ro02104 is a critical gene for determining the size of LDs. We then compared the TAG content of the ro02104 deletion mutant with that of WT. Interestingly, the TAG content in the mutant strain was slightly lower than that of the WT at the beginning, but was slightly higher later (Fig. 5B). As mentioned above, ro02104 belongs to the apolipoprotein family and may therefore protect LDs from fusion. For this reason, we hypothesized that its function is to protect LDs from fusion and named it microorganism lipid droplet small (MLDS).

The N-terminal of MLDS is required for targeting to LDs

Because deletion of MLDS resulted in supersized LDs, we investigated how it interacts with LDs. Bearing in mind its secondary structure and its similarity to apolipoproteins, we generated GFP-fusion proteins of MLDS truncation proteins of different sizes (truncated from the C-terminal). We then expressed these truncation mutants (amino acids 1–82, 1–146, 1–174, and 1–232) and the full-length protein in an MLDS deletion mutant (**Fig. 6A**). Signals in Western blotting with anti-GFP antibody indicated that the fusion proteins were successfully expressed, and no free GFP was detected (Fig. 6B). Analysis by confocal microscopy showed that the full-length, 1–232, 1–174, and 1–146 fragments colocalized with LDs, whereas the 1–82 fragment aggregated in the cytosol (Fig. 6C), indicating that the N-terminal 83–146 region is necessary for the targeting of MLDS to LDs.

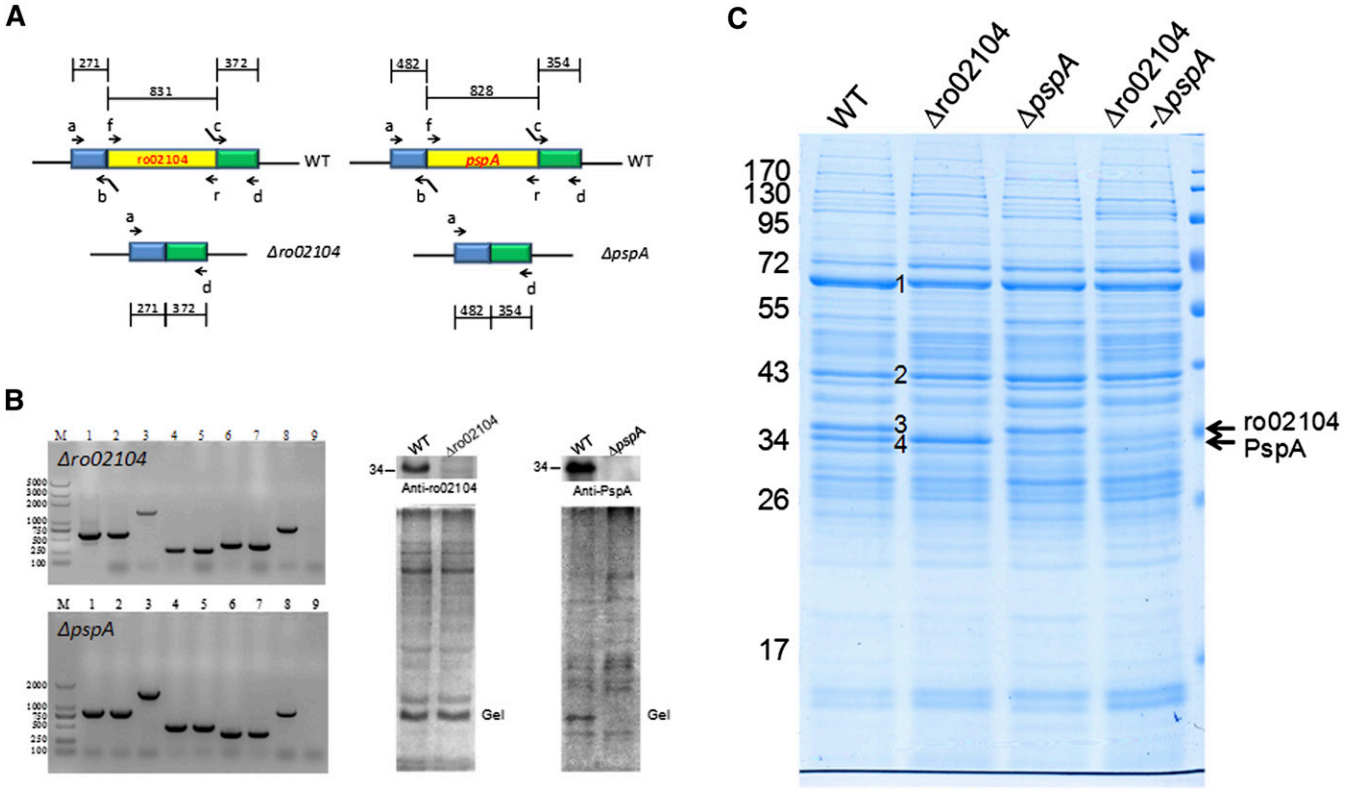

Fig. 4. Gene deletion demonstrates that ro02104 and PspA are two of the major proteins of lipid droplets. A: The diagrams show in-frame deletions of ro02104 and *pspA*. The detailed construction and screening process were described (see supplementary Fig. II). B: The left panel shows PCR confirmation of the deletion mutants. 1–3, Target gene, including the upstream and downstream fragments, amplified using the mutagenic plasmid, or genomic DNA of the deletion mutant or WT as the template and primers a and d; 4–5, the region upstream of the target gene amplified using genomic DNA of the WT or the deletion mutant as the template and primers a and b; 6–7, the downstream region of the target gene amplified using genomic DNA of the WT or deletion mutant as the template and primers c and d; 8–9, the target gene from the WT and the deletion mutant amplified using genomic DNA of the WT or the deletion mutant as the template and primers f and r. The right two panels show the Western blotting results that verify the ro02104 and *pspA* deletion mutants. C: LD proteins were extracted from the WT, ro02104 mutant, *pspA* mutant, and ro02104-*pspA* double-deletion mutant, and separated by 10% SDS-PAGE followed by Colloidal Blue staining. The main LD protein bands are labeled 1, 2, 3 (ro02104), and 4 (PspA).

DISCUSSION

Using a potential biofuel-producing bacterium *Rhodococcus* sp. RHA1 as a model, we provide biochemical and morphological evidence demonstrating that the long-observed structures in RHA1 are homologous to the lipid droplets of eukaryotic organisms. The comprehensive proteome of prokaryotic LDs and mutagenesis of LD-associated proteins identify two major LD proteins, including one putative structural protein that is an apolipoprotein-like protein, suggesting that apolipoproteins may have an evolutionarily conserved role in the storage and trafficking of neutral lipids.

Using a modified version of our previous method (12, 18), we isolated cellular structures (Fig. 1C) that floated on top of the sucrose gradient after ultracentrifugation and found that they had a shape similar to that of eukaryote LDs (Fig. 1A, D). Their similar density and highly enriched TAG content (Fig. 1F, G) suggested that they are similar to LDs. Our demonstration using Lipid-TOX staining and localizing MLDS on the surface of these structures (Fig. 6C) further confirmed their identity. TLC analysis of the lipid composition of LDs and total membrane lipids showed that in addition to large quantities of TAG, LDs possess a small amount of DAG and PE (Fig. 1G), indicating the purity of the LDs. The presence of DAG in LDs suggests that LDs may be involved in TAG metabolism. After characterization of the LD proteome, two major LD-associated proteins were identified: ro02104 and PspA. The predicted structure of ro02104 resembles that of apolipoproteins, the structural proteins of plasma lipoproteins. Deletion of ro02104 resulted in the formation of supersized LDs, suggesting that ro02104 plays a critical role in cellular LD dynamics. Our results suggest that apolipoproteins may have an evolutionarily conserved role in the storage and trafficking of neutral lipids.

Similar studies involving the isolation and proteomic analysis of lipid-containing granules/lipid inclusions from *Rhodococcus opacus* PD630 and *Rhodococcus ruber* have previously been carried out (42). When the lipid inclusions of these two bacteria were isolated, they were also found to contain a large number of proteins. However, when analyzed by SDS-PAGE, the proteomes of these isolated lipid inclusions closely resembled the proteomes of whole cells, even when sequential washing steps were included. A few of the most-predominant proteins were isolated and the

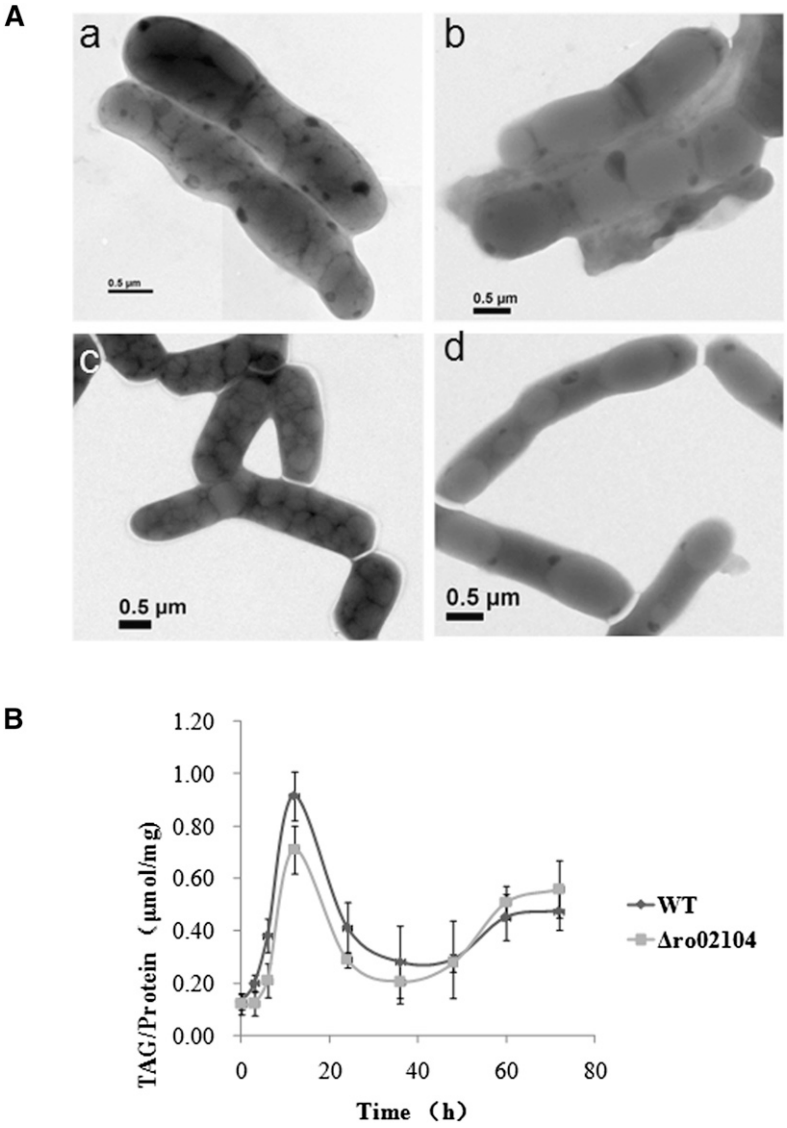

Fig. 5. Deletion of MLDS increases the size of lipid droplets. A: Cells of the WT RHA1, MLDS deletion mutant, *pspA* deletion mutant, and MLDS-*pspA* double-deletion mutant were cultivated in MSM for 24 h followed by negative staining and imaging by EM. A-a, WT; A-b, MLDS deletion mutant; A-c, *pspA* deletion mutant; A-d, MLDS-*pspA* double-deletion mutant; (bar = 0.5 μm). B: Identical quantities of cells of the WT and the MLDS deletion mutant were transferred to MSM from a preculture in NB. Bacteria were collected at the indicated time points. Bacterial samples were dissolved in 1% Triton X-100 by sonication after washing twice with PBS. Whole-cell lysates were then centrifuged at 10,000 *g* for 5 min at 4°C. The supernatant was transferred to a new tube for analysis. TAG levels were measured using an E1003 triglyceride assay kit (Applygen Technologies, China). Protein samples were quantified using a Pierce BCA Protein Assay Kit (Thermo, USA). Error bars indicate SD.

N-terminal amino acid sequences were determined. However, the function of these proteins was not determined (42). MALDI/TOF analysis was not meaningful at that time, because the genomes of both bacteria had not been sequenced.

The number of LD-associated proteins identified in this study falls within the range of previously reported proteomic studies of LDs from other sources (18), but their composition is unique. First, about 60% of the proteins were identified as metabolism-related enzymes, most of which are directly involved in lipid and glucose metabolism. The percentage of proteins involved in these functions was higher than that found in LDs from mammalian cells, indicating that LDs are metabolic centers in RHA1. Second, in comparison with LDs from mammalian cells, fewer trafficking proteins were found in the proteome of the LDs investigated in this study. This may be because, unlike eukaryotic cells, bacterial cells have a comparatively simple structure, and there is no need for trafficking between various kinds of organelles. Third, DNA polymerase and proteins related to cell division were also detected on LDs. Fourth, gene expression may occur on the surface of LDs since a number of transcriptional regulators and ribosomal proteins were identified in the proteome of LDs. Taken together, our proteomic data suggest that the lipid droplet surface provides a suitable membrane-like environment that might facilitate various molecular processes.

Although LDs are found in organisms from bacteria to humans, the major LD structural proteins, the PAT family (recently renamed PLINs), has only been identified in *Drosophila* and higher organisms. In order to use prokaryotic cells and *C. elegans* as model systems to study LD biology, it is important to know what LD major/structural proteins are present in the organisms. Our present work is the first to identify two major proteins of bacterial LDs, one of which, MLDS, may play a critical role in controlling LD size. Of significant interest, it is a mammalian apolipoprotein-like protein and possesses functions similar to those of its mammalian counterpart. Interestingly, MLDS was not similar to another apolipoprotein family, SAAs (43). We and other groups have found that some apolipoproteins are associated with LDs in mammalian cells, including apoA1/A4/A5/E (44–46), suggesting that MLDS may function as a structural protein in bacterial LDs.

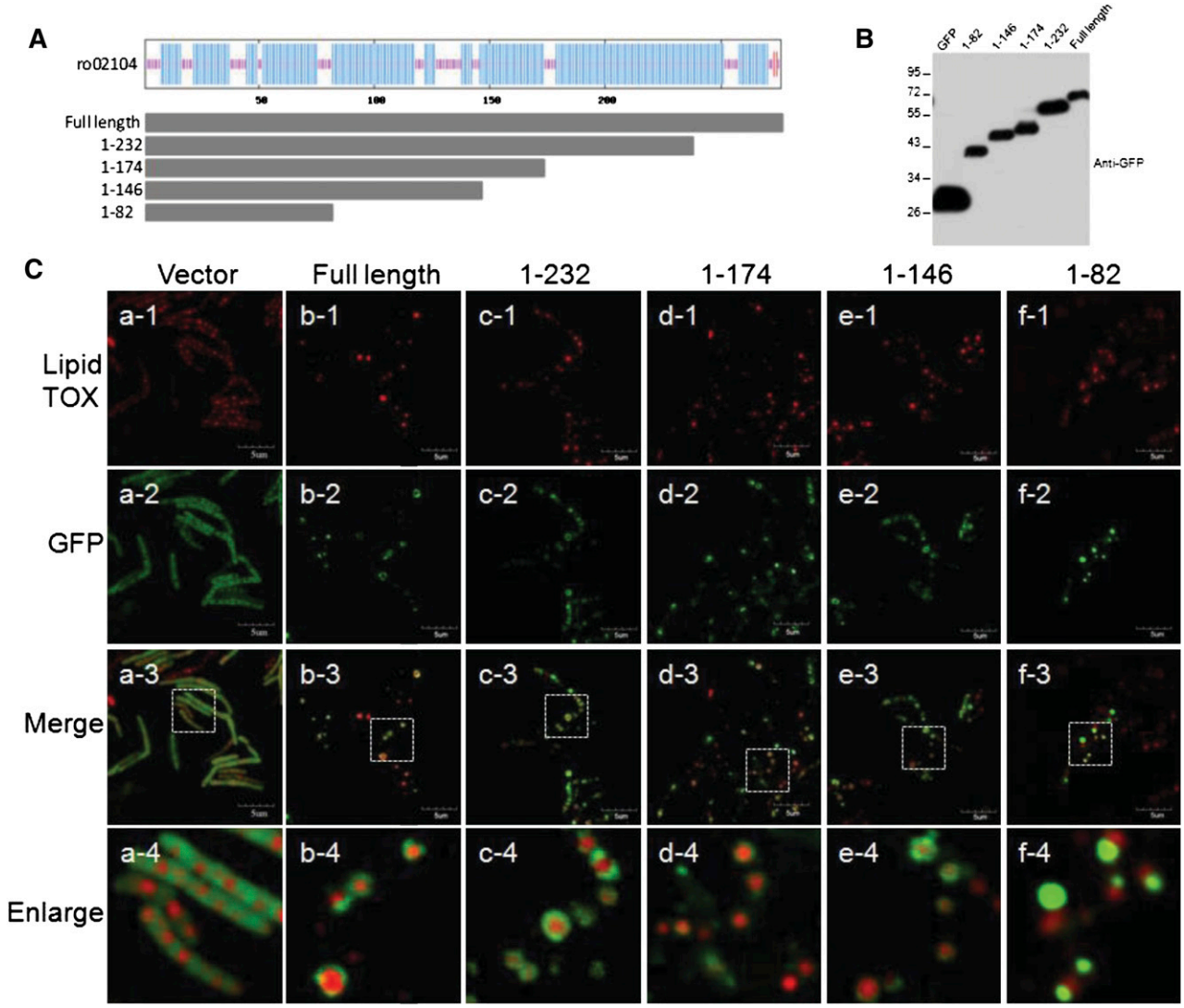

Fig. 6. The N-terminal is required for MLDS targeting to LDs. A: The full-length and truncation mutant proteins (1–232, 1–174, 1–146, and 1–82, designed according to the secondary structure of MLDS) were overexpressed in an MLDS deletion mutant strain after in-frame fusion with *egfp* in a pJAM-*egfp* expression vector. The blue regions represent α-helices. B: Single colonies were picked and cultivated in MSM. Western blotting shows successful expression of these fusion proteins by anti-GFP. C: Confocal images of different truncation mutants. MLDS mutant cells overexpressing different truncation mutants were cultivated in MSM for 24 h, followed by washing twice with PBS. Slides were viewed with an Olympus FV1000. a1–a4, JAM2-*egfp* overexpression; b1–b4, overexpression of full-length MLDS; c1–c4, overexpression of MLDS 1–232; d1–d4, overexpression of MLDS 1–174; e1–e4, overexpression of MLDS 1–146; f1–f4, overexpression of MLDS 1–82 (bar = 5 μm).

Previous studies have shown that a variety of proteins and lipids are involved in the regulation of LD size (47–50). Our EM data show that LDs become much larger and the number of LDs is markedly reduced in MLDS deletion mutant cells (Fig. 5A). On the basis of our data, we believe that regulation of LD fusion may involve proteins whose role is to block fusion in order to maintain appropriate-sized LDs. Cells may control LD size using this and other regulatory mechanisms in order to maintain their physiological functions.

TadA, a gene that is homologous to MLDS in *R. opacus* PD630, has been studied recently by Maceachran, Prophete, and Sinskey (51). Their *tad*A mutant generated by transposon mutagenesis had a lower TAG content and smaller LDs than the MLDS deletion mutant generated in this study. The discrepancy between these two studies may be due to differences between these two bacterial strains and the mutagenesis strategy used.

The physiological importance of LDs and the strong correlation between aberrant lipid storage and metabolic diseases highlights the need for further research on this organelle, including its biogenesis, growth, fusion, fission, movement, interaction with other cellular organelles, and biological function. Although recent proteomic studies and RNAi screening have provided much information (52, 53), the molecular mechanism that regulates LD biogenesis still remains elusive. Our proteomic analysis has identified not only many neutral lipid biosynthesis enzymes but also many membrane proteins, such as PspA (GI: 111023715), that seem to be involved in membrane stability. PspA forms

hollow spherical scaffold-like basal units in *E Escherichia coli* that combine to form a net structure on the membrane (54), suggesting that it may stabilize LD membrane in RHA1.

In summary, the present study has demonstrated the existence of prokaryotic LDs unequivocally for the first time and provides important additional insights into the molecular mechanisms governing LD biogenesis/dynamics. The knowledge gleaned from bacterial research will not only help answer fundamental questions about LD biogenesis and structure, but will also facilitate industrial applications such as improving the production of biodiesel using a more-robust bacterial strain.

The authors would like to thank Dr. Joy Fleming for her critical reading of this manuscript and useful suggestions. The authors are also grateful for Dr. Shufeng Sun's assistance with transmission electron microscopy.

REFERENCES

1. Fujimoto, T., Y. Ohsaki, J. Cheng, M. Suzuki, and Y. Shinohara. 2008. Lipid droplets: a classic organelle with new outfits. *Histochem. Cell Biol.* **130:** 263–279.
2. Farese, R. V., Jr., and T. C. Walther. 2009. Lipid droplets finally get a little R-E-S-P-E-C-T. *Cell.* **139:** 855–860.
3. Martin, S., and R. G. Parton. 2006. Lipid droplets: a unified view of a dynamic organelle. *Nat. Rev. Mol. Cell Biol.* **7:** 373–378.
4. Murphy, D. J. 2001. The biogenesis and functions of lipid bodies in animals, plants and microorganisms. *Prog. Lipid Res.* **40:** 325–438.
5. Zehmer, J. K., Y. Huang, G. Peng, J. Pu, R. G. Anderson, and P. Liu. 2009. A role for lipid droplets in inter-membrane lipid traffic. *Proteomics.* **9:** 914–921.
6. Goodman, J. M. 2008. The gregarious lipid droplet. *J. Biol. Chem.* **283:** 28005–28009.
7. Murphy, S., S. Martin, and R. G. Parton. 2009. Lipid droplet-organelle interactions; sharing the fats. *Biochim. Biophys. Acta.* **1791:** 441–447.
8. Zhang, S., Y. Du, Y. Wang, and P. Liu. 2010. Lipid droplet—a cellular organelle for lipid metabolism. *Acta Biophys Sin.* **26:** 97–105.
9. Maeda, K., H. Cao, K. Kono, C. Z. Gorgun, M. Furuhashi, K. T. Uysal, Q. Cao, G. Atsumi, H. Malone, B. Krishnan, et al. 2005. Adipocyte/macrophage fatty acid binding proteins control integrated metabolic responses in obesity and diabetes. *Cell Metab.* **1:** 107–119.
10. Miyanari, Y., K. Atsuzawa, N. Usuda, K. Watashi, T. Hishiki, M. Zayas, R. Bartenschlager, T. Wakita, M. Hijikata, and K. Shimotohno. 2007. The lipid droplet is an important organelle for hepatitis C virus production. *Nat. Cell Biol.* **9:** 1089–1097.
11. Fei, W., H. Wang, X. Fu, C. Bielby, and H. Yang. 2009. Conditions of endoplasmic reticulum stress stimulate lipid droplet formation in Saccharomyces cerevisiae. *Biochem. J.* **424:** 61–67.
12. Liu, P., Y. Ying, Y. Zhao, D. I. Mundy, M. Zhu, and R. G. Anderson. 2004. Chinese hamster ovary K2 cell lipid droplets appear to be metabolic organelles involved in membrane traffic. *J. Biol. Chem.* **279:** 3787–3792.
13. Brasaemle, D. L., G. Dolios, L. Shapiro, and R. Wang. 2004. Proteomic analysis of proteins associated with lipid droplets of basal and lipolytically stimulated 3T3-L1 adipocytes. *J. Biol. Chem.* **279:** 46835–46842.
14. Martin, S., K. Driessen, S. J. Nixon, M. Zerial, and R. G. Parton. 2005. Regulated localization of Rab18 to lipid droplets: effects of lipolytic stimulation and inhibition of lipid droplet catabolism. *J. Biol. Chem.* **280:** 42325–42335.
15. Ozeki, S., J. Cheng, K. Tauchi-Sato, N. Hatano, H. Taniguchi, and T. Fujimoto. 2005. Rab18 localizes to lipid droplets and induces their close apposition to the endoplasmic reticulum-derived membrane. *J. Cell Sci.* **118:** 2601–2611.
16. Beckman, M. 2006. Cell biology. Great balls of fat. *Science.* **311:** 1232–1234.
17. Bartz, R., W. H. Li, B. Venables, J. K. Zehmer, M. R. Roth, R. Welti, R. G. Anderson, P. Liu, and K. D. Chapman. 2007. Lipidomics reveals that adiposomes store ether lipids and mediate phospholipid traffic. *J. Lipid Res.* **48:** 837–847.
18. Bartz, R., J. K. Zehmer, M. Zhu, Y. Chen, G. Serrero, Y. Zhao, and P. Liu. 2007. Dynamic activity of lipid droplets: protein phosphorylation and GTP-mediated protein translocation. *J. Proteome Res.* **6:** 3256–3265.
19. Khandelia, H., L. Duelund, K. I. Pakkanen, and J. H. Ipsen. 2010. Triglyceride blisters in lipid bilayers: implications for lipid droplet biogenesis and the mobile lipid signal in cancer cell membranes. *PLoS ONE.* **5:** e12811.
20. Smith, V. H., B. S. Sturm, F. J. Denoyelles, and S. A. Billings. 2010. The ecology of algal biodiesel production. *Trends Ecol. Evol.* **25:** 301–309.
21. Andersson, L., P. Bostrom, J. Ericson, M. Rutberg, B. Magnusson, D. Marchesan, M. Ruiz, L. Asp, P. Huang, M. A. Frohman, et al. 2006. PLD1 and ERK2 regulate cytosolic lipid droplet formation. *J. Cell Sci.* **119:** 2246–2257.
22. Cho, S. Y., E. S. Shin, P. J. Park, D. W. Shin, H. K. Chang, D. Kim, H. H. Lee, J. H. Lee, S. H. Kim, M. J. Song, et al. 2007. Identification of mouse Prp19p as a lipid droplet-associated protein and its possible involvement in the biogenesis of lipid droplets. *J. Biol. Chem.* **282:** 2456–2465.
23. Puri, V., S. Konda, S. Ranjit, M. Aouadi, A. Chawla, M. Chouinard, A. Chakladar, and M. P. Czech. 2007. Fat-specific protein 27, a novel lipid droplet protein that enhances triglyceride storage. *J. Biol. Chem.* **282:** 34213–34218.
24. Kadereit, B., P. Kumar, W. J. Wang, D. Miranda, E. L. Snapp, N. Severina, I. Torregroza, T. Evans, and D. L. Silver. 2008. Evolutionarily conserved gene family important for fat storage. *Proc. Natl. Acad. Sci. USA.* **105:** 94–99.
25. Thiele, C., and J. Spandl. 2008. Cell biology of lipid droplets. *Curr. Opin. Cell Biol.* **20:** 378–385.
26. Voss, I., and A. Steinbüchel. 2001. High cell density cultivation of *Rhodococcus opacus* for lipid production at a pilot-plant scale. *Appl. Microbiol. Biotechnol.* **55:** 547–555.
27. Schirmer, A., M. A. Rude, X. Li, E. Popova, and S. B. del Cardayre. 2010. Microbial biosynthesis of alkanes. *Science.* **329:** 559–562.
28. Singh, A., P. S. Nigam, and J. D. Murphy. 2011. Mechanism and challenges in commercialisation of algal biofuels. *Bioresour Technol.* **102:** 26–34.
29. McLeod, M. P., R. L. Warren, W. W. Hsiao, N. Araki, M. Myhre, C. Fernandes, D. Miyazawa, W. Wong, A. L. Lillquist, D. Wang, et al. 2006. The complete genome of *Rhodococcus* sp. RHA1 provides insights into a catabolic powerhouse. *Proc. Natl. Acad. Sci. USA.* **103:** 15582–15587.
30. Banerjee, A., R. Sharma, and U. C. Banerjee. 2002. The nitrile-degrading enzymes: current status and future prospects. *Appl. Microbiol. Biotechnol.* **60:** 33–44.
31. Larkin, M. J., L. A. Kulakov, and C. C. Allen. 2005. Biodegradation and *Rhodococcus*–masters of catabolic versatility. *Curr. Opin. Biotechnol.* **16:** 282–290.
32. Hernández, M. A., W. W. Mohn, E. Martinez, E. Rost, A. F. Alvarez, and H. M. Alvarez. 2008. Biosynthesis of storage compounds by *Rhodococcus jostii* RHA1 and global identification of genes involved in their metabolism. *BMC Genomics.* **9:** 600.
33. Yalan Du, Y. W., G. Peng, Z. Su, M. Xu, W. Feng, S. Zhang, Y. Ding, D. Zhao, and P. Liu. 2011. Reducing COD and BOD, as well as producing triacylglycerol by LDS5 grown in CTMP effluent. *Bioresources.* **6:** 3505–3514.
34. Miura, S., J. W. Gan, J. Brzostowski, M. J. Parisi, C. J. Schultz, C. Londos, B. Oliver, and A. R. Kimmel. 2002. Functional conservation for lipid storage droplet association among perilipin, ADRP, and TIP47 (PAT)-related proteins in mammals, Drosophila, and Dictyostelium. *J. Biol. Chem.* **277:** 32253–32257.
35. Rene Bartz, J. Z., and P. Liu. 2005. The new face of lipid droplets. *Prog. Biochem. Biophys.* **32:** 387–392.
36. Kalscheuer, R., M. Arenskötter, and A. Steinbüchel. 1999. Establishment of a gene transfer system for *Rhodococcus opacus* PD630 based on electroporation and its application for recombinant biosynthesis of poly(3-hydroxyalkanoic acids). *Appl. Microbiol. Biotechnol.* **52:** 508–515.
37. Jensen, L. J., M. Kuhn, M. Stark, S. Chaffron, C. Creevey, J. Muller, T. Doerks, P. Julien, A. Roth, M. Simonovic, et al. 2009. STRING

8–a global view on proteins and their functional interactions in 630 organisms. *Nucleic Acids Res.* **37:** D412–D416.
38. Huang da, W., B. T. Sherman, and R. A. Lempicki. 2009. Systematic and integrative analysis of large gene lists using DAVID bioinformatics resources. *Nat. Protoc.* **4:** 44–57.
39. Huang da, W., B. T. Sherman, and R. A. Lempicki. 2009. Bioinformatics enrichment tools: paths toward the comprehensive functional analysis of large gene lists. *Nucleic Acids Res.* **37:** 1–13.
40. van der Geize, R., G. I. Hessels, R. van Gerwen, P. van der Meijden, and L. Dijkhuizen. 2001. Unmarked gene deletion mutagenesis of kstD, encoding 3-ketosteroid Delta1-dehydrogenase, in *Rhodococcus erythropolis* SQ1 using sacB as counter-selectable marker. *FEMS Microbiol. Lett.* **205:** 197–202.
41. Sharp, J. O., C. M. Sales, J. C. LeBlanc, J. Liu, T. K. Wood, L. D. Eltis, W. W. Mohn, and L. Alvarez-Cohen. 2007. An inducible propane monooxygenase is responsible for N-nitrosodimethylamine degradation by *Rhodococcus* sp. strain RHA1. *Appl. Environ. Microbiol.* **73:** 6930–6938.
42. Kalscheuer, R., M. Wältermann, M. Alvarez, and A. Steinbüchel. 2001. Preparative isolation of lipid inclusions from *Rhodococcus opacus* and *Rhodococcus ruber* and identification of granule-associated proteins. *Arch. Microbiol.* **177:** 20–28.
43. Malle, E., A. Steinmetz, and J. G. Raynes. 1993. Serum amyloid A (SAA): an acute phase protein and apolipoprotein. *Atherosclerosis.* **102:** 131–146.
44. Wu, C. C., K. E. Howell, M. C. Neville, J. R. Yates III, and J. L. McManaman. 2000. Proteomics reveal a link between the endoplasmic reticulum and lipid secretory mechanisms in mammary epithelial cells. *Electrophoresis.* **21:** 3470–3482.
45. Shu, X., J. Chan, R. O. Ryan, and T. M. Forte. 2007. Apolipoprotein A-V association with intracellular lipid droplets. *J. Lipid Res.* **48:** 1445–1450.
46. Zhang, H., Y. Wang, J. Li, J. Yu, J. Pu, L. Li, S. Zhang, G. Peng, F. Yang, and P. Liu. 2011. Proteome of skeletal muscle lipid droplet reveals association with mitochondria and apolipoprotein a-I. *J. Proteome Res.* **10:** 4757–4768.
47. Fei, W., G. Shui, B. Gaeta, X. Du, L. Kuerschner, P. Li, A. J. Brown, M. R. Wenk, R. G. Parton, and H. Yang. 2008. Fld1p, a functional homologue of human seipin, regulates the size of lipid droplets in yeast. *J. Cell Biol.* **180:** 473–482.
48. Bell, M., H. Wang, H. Chen, J. C. McLenithan, D. W. Gong, R. Z. Yang, D. Yu, S. K. Fried, M. J. Quon, C. Londos, et al. 2008. Consequences of lipid droplet coat protein downregulation in liver cells: abnormal lipid droplet metabolism and induction of insulin resistance. *Diabetes.* **57:** 2037–2045.
49. Fei, W., G. Shui, Y. Zhang, N. Krahmer, C. Ferguson, T. S. Kapterian, R. C. Lin, I. W. Dawes, A. J. Brown, P. Li, et al. 2011. A role for phosphatidic acid in the formation of "supersized" lipid droplets. *PLoS Genet.* **7:** e1002201.
50. Murphy, S., S. Martin, and R. G. Parton. 2010. Quantitative analysis of lipid droplet fusion: inefficient steady state fusion but rapid stimulation by chemical fusogens. *PLoS ONE.* **5:** e15030.
51. Maceachran, D. P., M. E. Prophete, and A. J. Sinskey. 2010. The *Rhodococcus opacus* PD630 heparin-binding hemagglutinin homolog TadA mediates lipid body formation. *Appl. Environ. Microbiol.* **76:** 7217–7225.
52. Ashrafi, K., F. Y. Chang, J. L. Watts, A. G. Fraser, R. S. Kamath, J. Ahringer, and G. Ruvkun. 2003. Genome-wide RNAi analysis of Caenorhabditis elegans fat regulatory genes. *Nature.* **421:** 268–272.
53. Guo, Y., T. C. Walther, M. Rao, N. Stuurman, G. Goshima, K. Terayama, J. S. Wong, R. D. Vale, P. Walter, and R. V. Farese. 2008. Functional genomic screen reveals genes involved in lipid-droplet formation and utilization. *Nature.* **453:** 657–661.
54. Standar, K., D. Mehner, H. Osadnik, F. Berthelmann, G. Hause, H. Lünsdorf, and T. Brüser. 2008. PspA can form large scaffolds in *Escherichia coli*. *FEBS Lett.* **582:** 3585–3589.